Fatigue of as-welded and stress relieved tubular T-joints

Autor(en): **Shinners, C.D. / Abel, A.**

Objekttyp: **Article**

Zeitschrift: **IABSE reports = Rapports AIPC = IVBH Berichte**

Band (Jahr): **37 (1982)**

PDF erstellt am: **16.07.2024**

Persistenter Link: https://doi.org/10.5169/seals-28979

Fatigue of As-Welded and Stress Relieved Tubular T-Joints

Fatigue de branchements en T tubulaires soudés, recuits ou non

Ermüdung von unbehandelten und spannungsfrei geglühten, geschweissten T-Rohrverbindungen

C.D. SHINNERS
Engineer
Esso Australia
Sydney, Australia

A. ABEL
Associate Professor
The University of Sydney
Sydney, Australia

SUMMARY
As-welded and stress relieved large scale tubular T-joints were tested under static and dynamic loading. Strain distributions at the hot spots are presented and compared in relation to the specimen dimensions. Stress relieving was found to enhance fatigue performance with respect to both the cycles to crack initiation and failure. The complex crack propagation behaviour is also discussed.

RESUME
Des pièces de branchement en T tubulaires de grande dimension, en acier soudé, recuit ou non, ont été testées sous des charges statiques et dynamiques. Les distributions des déformations relatives aux endroits critiques sont montrées et sont comparées en relation avec les dimensions de l'échantillon. On a constaté qu'un recuit pour supprimer les contraintes résiduelles avait un effet favorable sur les caractéristiques de fatigue, aussi bien pour le nombre de cycles correspondant à l'apparition d'une fissure que pour celui correspondant à la rupture. Le comportement complexe durant la phase de propagation des fissures est également discuté.

ZUSAMMENFASSUNG
Geschweisste T-Verbindungen von Rohren mit grossen Abmessungen wurden unter statischer und dynamischer Belastung geprüft. Dies erfolgte sowohl mit unbehandelten als auch mit wärmebehandelten Prüfkörpern. Die Dehnungsverteilung an den gefährdeten Stellen wird aufgezeigt und in Verbindung mit den Dimensionen der Prüfkörper verglichen. Es hat sich gezeigt, dass die Wärmebehandlung das Ermüdungsverhalten verbessert und zwar im Stadium des Rissbeginns wie auch beim Ermüdungsbruch. Die komplexe Phase der Rissfortpflanzung wird ebenfalls behandelt.

1. INTRODUCTION

The deployment of welded tubular structures for the recovery of offshore crude oil has lead to much needed research into the static and dynamic load behaviour of the fatigue prone tubular joints. Such joints are susceptible to fatigue simply as a welded joint but more importantly because of the coincidence of regions of local stress concentration, known as hot spots, with the weld line.

Fatigue lives in air will largely be governed by hot spot strain magnitude and the condition of welding. For this reason methods of estimating hot spot strains in actual joints and theoretical models have been developed, and post weld processes, for example grinding, have been investigated as possibilities for improving fatigue life. It is along these lines that three as-welded and two stress relieved T-joints were statically and cyclically loaded to investigate the influence of joint geometry on strain distributions and fatigue lives, as well as the possible fatigue performance enhancement by stress relieving, known in the case of small specimen welds.

2. EXPERIMENTAL DETAILS

2.1 Specimens

Five T-joint specimens were tested under axial brace loading as shown in Fig. 1. This figure also shows the adopted convention for stress-strain dimensions. The dimensions of the tubulars, as well as the parameters typically used to define joint geometry are given in Table 1. On the basis of the test programme the following five comparisons can be made:

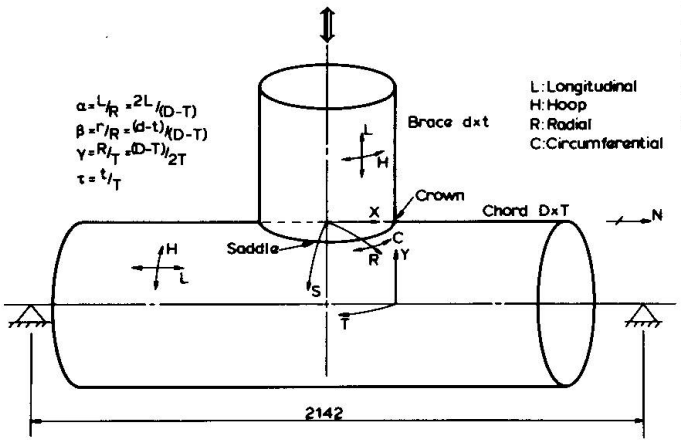

Fig. 1 Specimen Configuration

Specimens:

- 1 (as welded) and 2 (stress relieved)
- 1 and 3 (thinner chord wall)
- 1 and 4 (smaller chord diameter)
- 4 (as welded) and 5 (stress relieved)
- 2 and 5 (smaller chord diameter)

Specimen	Condition	D	T	d	t	α	β	γ	τ
1	AW(1)	610	19.7	406	9.7	7.26	0.67	15.0	0.49
2	SR(2)	610	19.7	406	9.7	7.26	0.67	15.0	0.49
3	AW	610	12.3	406	9.7	7.17	0.66	24.3	0.79
4	AW	508	19.4	406	9.7	8.76	0.81	12.6	0.50
5	SR	508	19.4	406	9.7	8.76	0.81	12.6	0.50

(1) As Welded (2) Stress Relieved

Table 1 Specimen Details

2.2 Materials, Welding and Post-Weld Heat Treatment

The seamed tubulars were rolled from steel designated AB3603, according to Australian Iron and Steel Company terminology, developed for offshore platforms in Bass Strait, Australia. Tensile properties of the steel are provided in Table 2.

	Yield Strength MPa	Ult. Strength MPa	% Reduction of area	% Elongation in $5.65\sqrt{S_0}$
Specified	250 Min	410 Min	-	22 Min
Measured (1)	244,244(3)	382	76	40
(2)	244,340	458	58	34

(1) Tube longitudinal direction.

(2) Tube circumferential direction after flattening of tube.

(3) Second value represents 0.2% proof stress

Table 2 Tensile Properties of AB3603

A manual-metal-arc welding method was used by the fabricators with experience in the offshore industry. Welding preparation and procedures were according to AWS Structural Welding Code D1.1-72 with the exception that a single weld run was deposited from inside the brace.

The following post-weld heat treatment procedure was used in the case of specimens 2 and 5: heating at 100°C/hr, hold for 1 hour between 580 and 620°C, cooling at 150°C/hr to 300°C, followed by air cooling.

2.3 Strain Gauging and Instrumentation

All specimens were strain gauged around the weld line on both the brace and chord inside and outside surfaces. At the saddle positions gauges were attached radiating from the weld toe on the chord side to enable determination of hot spot stresses and strains by extrapolation. Combinations of rosette gauges, strain gradient gauges and single element gauges were used. The rosettes were necessary for determining stress distributions in the biaxial stress fields existing around the weld line. Symmetrical gauges, specifically higher up the brace, permitted a check of specimen alignment and axiality of loading. Specimen 1 was also monitored with a large number of rosettes attached away from the weld line in order to improve on the gauge positioning for the subsequently tested specimens.

2.4 Crack Growth Monitoring

Crack initiation was detected through monitoring of strain behaviour adjacent to the weld toe at the hot spots. Visual observation and confirmation of the crack was aided by a low power magnifying glass and a highly volatile solvent which, when applied to the specimen surface under dynamic loading, bubbled in the vicinity of a crack. The same technique was used for surface crack growth measurements.

Crack marking provided information about through thickness crack growth in specimens 2 to 5 and ultrasonic techniques were tried in the case of specimens 1 and 2. In specimens 2 to 5 a combination of appropriately placed "sacrificial" strain gauges and specially developed crack propagation gauges were used. A constant current was applied to the gauges consisting of a parallel multi wired

arrangement so that a wire breaking was detected by a change in voltage across the gauge.

2.5 Experimental Procedure

Initially each specimen was subjected to two incremental static load cycles, between which, specimen alignment was adjusted and hot spot strain amplitudes were checked. This was followed by fully reversed (R = -1) sinusoidal dynamic loading which was interrupted periodically to monitor all strain gauges under static loading.

The load amplitudes, directed towards high cycle fatigues were selected to achieve the same hot spot strain amplitude for each specimen.

3. STATIC RESULTS

3.1 Strain Distributions

Figure 2 shows the radial strain distribution along the chord S-axis for specimens 1, 3 and 4. In plotting only one side, symmetrical gauges have been averaged. The distributions have been plotted as the ratio of measured strains to the nominal brace membrane strain, ε_{NOM}, for each specimen. This is calculated from $\varepsilon_{NOM} = (P/Ab)/E$ where P is the axial load and Ab is the cross-sectional area of the brace wall.

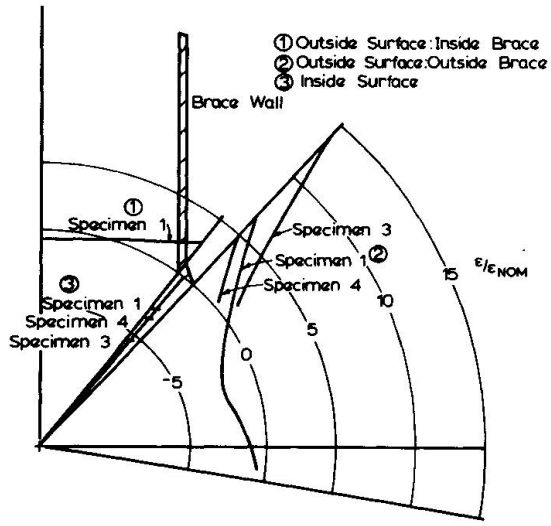

Fig. 2 Radial Strain Distribution in Chord along S-axis: Specimens 1, 3 and 4

For the joint and loading configuration investigated, the normalised strains typically correspond to the maximum principal strains, the principal stress direction on the chord surface being radial to the brace. This is not the case within the restraining brace where the maximum strains, at the top centre of the chord, correspond closely to the (maximum) nominal bending strains and hence are aligned in the longitudinal direction. Figure 2 clearly shows the existence of the hot spot or area of stress concentration at the saddle weld toe. The effect of a reduction in chord wall thickness is seen to produce a much steeper strain gradient approaching the weld toe and, comparing inside and outside surface strains, a higher contribution of membrane strain. A reduction in chord diameter has done little to the strain gradient and simply produced an overall reduction in strain concentration. The contribution of membrane strains is seen to be very low.

3.2 Stress-Strain Concentration

The ratio of hot spot strains to the nominal brace strains can be seen to be highest for specimen 3 and lowest for specimen 4. Normally the hot spot stresses/strains used to calculate stress-strain concentration factors (SCF's/SNCF's) are those existing at the weld toe but not influenced by local weld geometry or microscopic defects such as pits or cracks. In tubular joint specimens they have been determined either by linear extrapolation from two gauge readings [e.g. 1] or curved extrapolation from a number of readings [e.g. 2] taken radially to the

intersection line. Curve fitting in this case is generally done by eye. Linear extrapolation was proposed as a means of reducing the subjectivity involved with curve fitting in a region of such steep strain gradient. The recommended gauge locations for linear extrapolation have varied in the past but typically have been defined by a distance from the weld toe given by some function of $\sqrt{RT}$ or $\sqrt{rt}$ for the brace or chord respectively. To avoid weld toe influences a minimum distance to the closest gauge was originally set at 4 mm [3], although more recently 0.4T was concluded to be the limit of influence [4].

In Table 3, SCF's and SNCF's are given for the brace and chord saddle of specimen 4 as well as actual and recommended reading points for linear extrapolation. This Table shows the effect of linear extrapolation in significantly reducing

	CHORD		BRACE	
	SCF/SNCF	Extrapolation points	SCF/SNCF	Extrapolation points
SCF Curve	5.8			
Linear 1	5.2	$0.4T, 0.2\sqrt{RT} + 5°$	4.6	$0.2\sqrt{rt}, 1.4\sqrt{rt}$
Linear 2	5.4	$0.4T$, 5°		
SNCF Curve	4.7		4.9	
Linear 1	4.2	$0.4T, 0.2\sqrt{RT} + 5°$	3.7	$0.2\sqrt{rt}, 1.4\sqrt{rt}$
Linear 2	4.4	$0.4T$, 5°	4.1	$0.2\sqrt{rt}, 0.65\sqrt{rt}$
Recommended (2)		(1) $0.2\sqrt{RT}, 0.2\sqrt{RT} + 5°$		$0.2\sqrt{rt}, 0.65\sqrt{rt}$
(5&6)		$0.4T$, 5°		$0.2\sqrt{rt}, 0.65\sqrt{rt}$
Predicted SCF				
Wordsworth (7)	5.1, 4.9 (2)		4.2, 4.1 (2)	
Kuang (3) (8)	3.6		4.8	
Teyler (9)	4.0		5.0	

(1) Minimum set at 4 mm

(2) Corrected for weld leg length

(3) $\beta = 0.81$, Formulae valid $\beta < 0.8$

Table 3 SCF's/SNCF's for Specimen 4: Saddle Position

estimated SCF's and SNCF's in both the brace and chord. The difference between the linearly extrapolated values is not high but this would be influenced by the fact that the same "closest" reading was used in each case, namely that at 0.4T. If the previously recommended $0.2\sqrt{RT}$ had been used in the case of the chord, as was done for the brace, then the corresponding values for the SCF and SNCF would have been even lower.

A comparison with the predictions for the SCF's from the formulae of Wordsworth and Smedley [6], Kuang et al. [7] and Teyler et al. [8] is also given in Table 3. For this specimen, the "uncorrected" formulae of Wordsworth and Smedley, obtained from acrylic model studies, is seen to provide the most accurate prediction for the chord SCF. The formulae of Teyler et al., obtained from curved thin shell finite element studies, agree best with the brace SCF. It should be noted however that the brace SCF was obtained only from linear extrapolation and therefore would be lower than the "actual" SCF. The chord SCF obtained by curved extrapolation in specimen 5 was 5.0, as opposed to 5.8 for specimen 4, and this former value agrees very well with the prediction of Wordsworth and Smedley.

4. DYNAMIC RESULTS

4.1 Influence of Stress Relieving

As described above, crack initiation was detected using both strain monitoring and visual observation. Failure was defined by a rapid increase in joint deflection. Table 4 provides the fatigue results of all specimens in terms of the number of cycles to crack initiation and failure as functions of the hot spot strain ranges. These were determined using full extrapolation to the weld toe of strain measurements under both tensile and compressive loading, and then summing the two. Data is provided for both the east and west sides for each joint

Specimen	$\Delta\varepsilon_{Hot\ Spot}$		East		West		N_f
	E	W	N_c (1)	N_c (2)	N_c (1)	N_c (2)	$\times 10^6$
1	777	820	0.332 (3)	0.1	0.32 (3)	0.1	2.55
2	738	835					20
2	1494	1645	0.1	0.05	0.05	0.04	0.6
3	793	765	0.45	0.4 (4)	0.45	0.5	1.55
4	738	789	0.087	0.05	0.056	0.04	0.941
5	685	690	3.25	2.5	3.8	5.0	9.07

(1) Visual observation

(2) Strain drop at hot spot under tensile load

(3) Crack length > 80 mm, i.e. initiation missed

(4) Strain redistribution as crack initiation site not coincident with strain gauge

Table 4 Fatigue Data for all Specimens

As can be seen from the Table, specimen 2 did not show any signs of fatigue damage after 20 million load cycles. At this stage cycling was recommenced at twice the load amplitude. A comparison of specimens 1 and 2, and 4 and 5 indicates the beneficial effect of stress relieving in terms of improvement in both cycles to crack initiation and cycles to failure.

The thin walled specimen 3 showed a superior life to crack initiation. This is probably in line with the dimensional influence on fatigue strength observed elsewhere [9]. The fact that the fatigue life was not superior to that of the other specimens suggests that it was not necessarily a simple thickness effect but differences in residual stress states may also be involved.

Using the strain indicated crack initiation data, and the hot spot strain data for the joint side to indicate first cracking, the results of Table 4 have been plotted in Fig. 3 to further show the influence of the stress relieving. Also shown in Fig. 3 is the as-welded and stress relieved fatigue data of Yamaski et al. [11] who concluded that stress relieving had no influence on fatigue strength. Although statistically not sifgnificant two of their specimens tested at the same load range clearly show a superior fatigue strength for the stress relieved specimen. One futher remark about the cited work is that most of the specimens were tested at higher strain ranges at which the influence of residual stresses will be reduced.

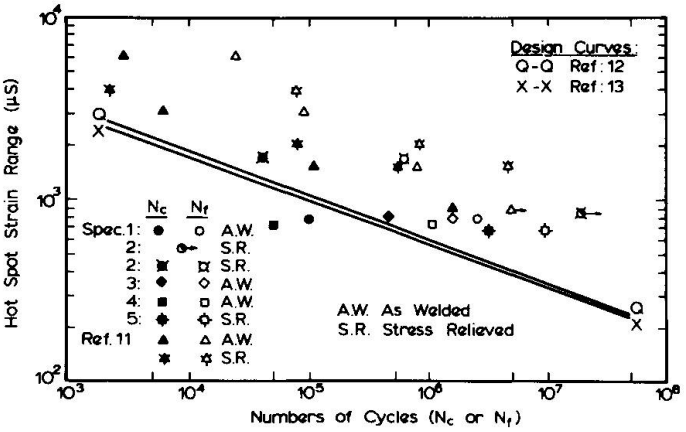

Fig. 3 Comparison of As Welded and Stress Relieved Fatigue Data

Two appropriate tubular joint design curves, from the Department of Energy [Q-Q curve, Ref. 12] and the American

Petroleum Institute (X-X curve, Ref. 13), drawn on Fig. 3 indicate conservatism with regard to failure for these specimens but not in terms of crack initiation.

4.2 Crack Propagation

In all specimens crack initiation occurred in the vicinity of the hot spots of the chord side weld toe. Crack propagation continued simultaneously around the weld toe and into the chord wall. Loss of joint rigidity typically occurred when the surface cracks were approaching the crowns. Figure 4 shows the surface crack propagation in the as-welded specimen 1. This figure illustrates fairly symmetrical and uniform crack growth rates resulting from stress redistribution away from the higher stressed saddle towards the lower stressed crown [14]. Figure 4 also indicates crack branching on the east side, whereby secondary cracks propagated away from the chord wall towards the direction of the chord longitudinal axis. Crack growth rates for these secondary cracks can be seen to be significantly lower than for the weld toe crack.

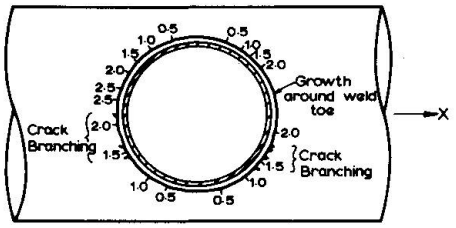

Fig. 4 Specimen 1: Crack Growth in Millions of Cycles

The crack path through the chord wall in specimen 1 is shown for the west saddle and near the north crown in Fig. 5. At the saddle four distinct stages of propagation can be identified following initiation at the weld toe. Stage 1 growth was normal to the chord surface and continued to a depth of about 2-3 mm to the limit of the heat affected zone. This type of growth extended the full length of the crack and the surface was generally smooth and flat. At the saddle the growth then changed direction to being normal to the brace axis, stage 2. This indicates a triaxial stress state with maximum stresses arising directly from the brace-chord load transfer rather than the resulting chord wall bending. The surface of this stage of growth was irregular and indicative of a combination of opening mode I and shear mode II type crack growths [15]. Mode II type growth tends to bring out the structural feature of the parent material. The third stage of growth, stage 3, was normal to the chord wall again and left a smooth surface. Increased bending stresses from the reduced wall thickness would have changed the crack growth direction. Eventually the remaining ligament was so small through cracking occurred with the formation of a shear lip, stage 4. Away from the saddles stage 2 growth was not evident and so chord wall bending (and membrane) stresses must have continually dominated. The above serves to illustrate the complex fatigue behaviour of tubular joints and the difficulty in applying techniques such as fracture mechanics to life prediction.

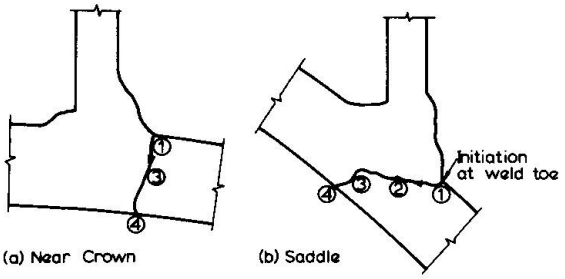

Fig. 5 Specimen 1: Through Wall Crack Paths

5. CONCLUSIONS

For large scale tubular T-joints subjected to static and dynamic axial brace loading,

- reduction of chord wall thickness significantly increased radial strain gradients at the saddle hot spots whilst reducing the chord diameter simply reduced the strain magnitudes without significantly affecting strain gradients,
- linear extrapolation techniques estimate stress and strain concentration factors that are significantly lower than those determined from curve fitting to more than two readings,
- stress relieving significantly improves the fatigue strength with regard to crack initiation and final failure, and
- through wall crack propagation paths varied around the weld toe circumference depending upon the developing stress states.

REFERENCES

1 DIJSTRA, O.D., de BACK, J.: Fatigue Strength of Tubular T- and X-Joints. Paper No. OTC3696, 12th Annual Offshore Technology Conf., Texas, May, 1980.
2 NOEL, J.S., BEALE, L.A., TOPRAC, A.A.: An Investigation of Stresses in Welded T-Joints. Report No. S.F.R.L. Tech. Rept. p. 550-3, Structures Fatigue Res. Lab., Dept. of Civil Engineering, The Univ. of Texas, 1963.
3 De BACK, J.: Report on Session 10, Testing of Tubular Joints. European Offshore Steels Select. Seminar, Cambridge, 1978.
4 WARDENIER, J.: Private Communication, May 1981.
5 WARDENIER, J.: Some New Developments in the Design of Large Metal Structures. Keynote Address: Metal Structures Conference, 1981, Newcastle (Aust.), Inst. of Engrs Aust., May, 1981.
6 WORDSWORTH, A.C., SMEDLEY, G.P.: Stress Concentrations at Unstiffened Tubular Columns. European Offshore Steel Select. Seminar, Cambridge, 1978.
7 KUANG, J.G., POLVIN, A.B., LEICK, R.D.: Stress Concentration in Tubular Joints. Paper OTC2205, 7th Annual Offshore Technology Conf., Texas, May, 1975.
8 TEYLOR, R., GILSZTEIN, M., BJØRNSTAD, H., HAUGAN, G.: Parametrical Stress Analysis of T-Joints. Det Norske Veritas, Report No. 77-523, November, 1977.
9 WYLDE, J.G., McDONALD, A.: The Influence of Joint Dimensions on the Fatigue Strength of Welded Tubular Joints. Int. J. Fatigue, Jan. 1980.
10 GURNEY, T.R.: Fatigue of Welded Structures. Snd Ed. Cambridge Univ. Press, Cambridge, 1979, Chap. 10.
11 YAMASAKI, T., TAKIZAWA, S., KOMATSU, M.: Static and Fatigue Tests on Large-Size Tubular T-Joints. Paper OTC3424, 11th Annual Offshore Technology Conf., Houston, Texas, May, 1979.
12 DEPARTMENT OF ENERGY: Offshore Installations: Guidance on Design and Construction. London, July, 1977.
13 AMERICAN PETROLEUM INSTITUTE: Recommended Practice for Planning, Designing and Constructing Fixed Offshore Platforms, APO RP2A, 11th Ed., Jan. 1980.
14 SHINNERS, C.D., ABEL, A.: Stress Analysis of Large Scale Tubular T-Joints. Symposium on Stress Analysis for Mechanical Design, 1981. The Institution of Engineers, Australia, National Conf. Publication No. 81/4.
15 DOVER, W.D., HOLDBROOK, S.J.: Fatigue Crack Growth in Tubular Welded Connections. Int. J. Fatigue, Jan. 1980.